RNA-ligand complexes and the attenuation of neutral confinement in the evolution of RNA secondary structures

Antonio Loreto*[1], Edgardo Ugalde[1], and Carlos Espinosa-Soto†[1]

[1]Instituto de Física, Universidad Autónoma de San Luis Potosí, Av. Parque Chapultepec 1570, San Luis Potosí, Mexico

December 18, 2025

Abstract

RNA molecules with identical nucleotide sequence can adopt different structures. Mutations can alter the properties of such structures; for example, some mutations increase the stability of a functionally relevant structure at the expense of other structures' stability. Interestingly, the structural diversity that a sequence produces is correlated to the number of structures that it can access upon mutation. Thus, enhancing a structure's stability can lead to neutral confinement, an evolutionary dead end in which mutational access to novel structures is increasingly difficult. If structure is critical to biological function, how do RNA molecules escape neutral confinement? We developed a model in which an RNA molecule's function depends on binding to a ligand and we applied it to study sequences that fold according to RNA biophysics, also simulating their evolution. We identified effects that decrease the selective advantage of augmenting a structure's stability. By disfavouring evolution of highly stable structures and favouring the accumulation of genetic variation, these effects hinder neutral confinement. The most important effect stems from the sequestration of high affinity structures in RNA-ligand complexes and their replenishment through thermal fluctuations. In this perspective, a common scenario may help to explain how RNA evolution avoids coming to a halt.

Keywords: RNA secondary structure | Neutral confinement | Conformational diversity | Conformational selection

*Present address: Genomics, Bioinformatics and Evolution Group, Departament de Genètica I Microbiologia, Universitat Autònoma de Barcelona, Cerdanyola del Vallès, Spain

†Corresponding author: carlos.espinosa@uaslp.mx

Introduction

After presumably playing a leading role in the early stages of evolution of life on Earth [1; 2], RNA molecules have diversified and acquired a wide range of cellular functions, some of them as fundamental as gene activity regulation, protein synthesis, gene expression, cell differentiation, response to infectious agents and many others [3; 4]. Since structure is critical to define a molecule's binding partners, many of RNA's functions depend substantially on the molecule's structure [5–17]. To a great extent, evolution of RNA molecules is the evolution of their structures.

Recent research supports that a cell's multiple copies of the same RNA sequence do not fold into the same molecular structure [7; 17–21]. The explanation is simple: one region of an RNA molecule may be able to bind, through Watson-Crick base-pairing, two or more distinct regions of the same molecule. Therefore, RNA molecules with exactly the same nucleotide sequence may adopt different structures. In thermodynamic equilibrium, the probability of finding a specific structure follows the Boltzmann distribution, increasing with the structure's stability [20–23]. Some such structural variants may not be able to perform the same functions as, for example, the sequence's minimum free-energy structure (MFES), which is the most stable and abundant structural configuration. Some may even be able to perform other functions that the molecules that adopt the MFES cannot perform [7; 17; 24].

One may be tempted to consider the ability of an RNA sequence to produce structural variation as an evolutionary asset; after all, secondary functions performed by low frequency structures could be the seed for the evolution of new biochemical abilities, as some have suggested for proteins [25–27]. However, an important and influential computational study on the evolution of RNA structures not only opposes this idea but also supports that such structural variation is indeed an evolutionary handicap [28]. In that study, Ancel and Fontana simulated the evolution of RNA considering a sequence's *plastic repertoire*, the set of structures that a sequence can fold into. They found that populations often failed to evolve the optimum structure. The reason stems from one of the authors' important observations concerning the plastic repertoire of a sequence s_i and its *mutational repertoire*, which comprises all the MFES in the set of sequences that differ from s_i by a single nucleotide substitution. They found that structures in the plastic repertoire of a sequence s_i often also appear in s_i's mutational repertoire and that the number of distinct structures in the two repertoires are positively associated. Ancel and Fontana refer to this association as *plastogenetic congruence*, as it shows that plastic effects, resulting from non-genetic perturbations like thermal fluctuations, are aligned with

genetic effects. Since then, multiple studies have supplemented statistical evidence for such plastogenetic congruence in RNA molecules [22; 29–33].

Ancel and Fontana assumed, correctly in our opinion, that fitness depends on each structure's ability to perform a function and on the amount of molecules that adopt such structure. Thus, in their model, a structure's contribution to fitness reflects how similar is that structure to a pre-defined optimal structure and its expected abundance, according to the Boltzmann distribution [28]. In these circumstances, mutation can increase fitness either by finding new structures more similar to the optimum or by increasing the thermodynamic stability of the better structures in the plastic repertoire. If, during their evolution, sequences encounter more often the latter kind of mutations, fitness would increase but it would do so at the expense of other structures in the plastic repertoire. After all, increasing the relative abundance of one structure implies diminishing that of others, eroding the plastic repertoire's structural diversity. Because of plastogenetic congruence, this comes at the cost of lower chances to access new better structures through mutation. Thus, selection leads to an evolutionary cul-de-sac in which a population is confined to sequences that yield the same MFES with a high thermodynamic stability and that have little mutational access to further improvement. Ancel and Fontana called this situation *neutral confinement* [23; 28; 34].

Given that RNA sequences yield large, diverse ensembles of structures and that RNA structure is typically crucial to a molecule's function, we wonder how RNA molecules have avoided the evolutionary dead-end alley that neutral confinement implies. Ancel and Fontana suggested that recombination of distinct RNA molecules could be a way out of neutral confinement [23; 28]. Indeed, recombination seems to be important in the evolution of genomes of RNA viruses [35; 36] and recombination of different RNA molecules could have been specially important in early evolution of life [37]. However, we consider unlikely that recombination suffices to solve the apparent paradox. Here we put forward an additional answer.

Neutral confinement occurs in the Ancel-Fontana model because there is a strong selective incentive to increase the stability of the RNA secondary structures associated to enhanced functional efficiency [28]. Conditions that abate such an incentive may make neutral confinement wane. We assumed that the function of an RNA molecule depends on binding to a ligand that, for simplicity, we consider that maintains a constant concentration. A cell's free RNA molecules with identical sequence may fold into any of several possible structures that differ in their ability to bind the ligand. Structures that better fit the ligand would form RNA-ligand complexes more easily. Remaining free RNA molecules, subject to thermal fluctuations, would convert randomly from one of the sequence's compatible structures to another, replenishing the pool of

RNA molecules that fold into structures best suitable for ligand binding. We hypothesized that, in this scenario, increasing a high affinity structure's stability would imply only a marginal evolutionary advantage: Consider the case in which structures with a high affinity for the ligand are not very stable. Even then, the sequestration of such structures in RNA-ligand complexes would impel other molecules to build up the stock of high affinity configurations. If this were the case, we may observe a significant attenuation of neutral confinement.

To evaluate the validity of our hypothesis, we developed a differential equations model that takes into account the structural diversity that an RNA sequence can produce, the thermal fluctuation-driven transitions from one structure in the plastic repertoire to another, and the dynamics of binding and unbinding of RNA and ligand molecules. We focused on secondary structures because this level of RNA structure description determines most of the molecule's stability [23; 38; 39], it provides the basic elements upon which tertiary structure assembles [6; 40; 41] and because we have access to computationally efficient tools and algorithms that, grounded in thermodynamics and RNA biophysics, allow us to predict a sequence's MFES and plastic repertoires [22; 42–44].

We studied first hypothetical simplified RNA molecules that only produce two structures in their plastic repertoire. We also studied RNA sequences that fold into specific biological or random structures as their MFES and in which only the rules of RNA folding define the properties of their plastic and mutational repertoires. Congruously with our hypothesis, when we consider explicitly ligand binding, fitness still increases monotonically with the thermodynamic stability of the optimal structure. However, a consistent increase in such stability results in diminishing fitness returns: as thermodynamic stability increases, the selective incentive to increase further thermodynamic stability fades. In addition, we identified conditions that enhance this effect. We also evaluated whether decreasing the fitness benefit that an increased RNA stability confers was sufficient to attenuate neutral confinement. To this end, we analysed evolutionary simulations in which selection favors sequences that are able to yield the greater equilibrium concentrations of RNA-ligand complex. In our simulations, evolution occurs in a stabilizing selection regime in which a population starts with the optimal phenotype and selection favors genetic variants that produce that phenotype more easily. The reason is that we considered that avoiding phenotypic evolutionary transitions would allow easier observation and analysis of neutral confinement. Specifically, evolution in our set-up initiates with RNA sequences that yield as their MFES a structure with maximum affinity for the ligand, albeit perhaps not with a very high thermodynamic stability. We found that mutational robustness and thermodynamic stability are evidently lower in

populations in which we consider explicitly ligand binding. In contrast, genetic variation within a population and the population's access to new structures through mutation and thermal fluctuations are greater in those populations. Therefore, our results support one scenario, that we expect to be widely common in nature, in which evolution of RNA secondary structures avoids the harshest effects of neutral confinement.

Methods

Sampling of sequences

We analyzed RNA sequences that fold into specific RNA secondary structures as their minimum free energy structures (MFES). We focused on five biologically relevant RNA structures that we obtained from the RNAcentral database [45] and ten additional structures that we identified as the MFES of random nucleotide sequences (Supplementary Tables ST1,2). The biological structures that we study include those of ribozymes, small nucleolar RNA, the transcriptional regulator DsrA and a tRNA. They are coded in mammalian, bacterial or viral genomes. We used the inverse-fold algorithm [46] in the ViennaRNA library [44] to sample randomly sequences that fold into one of these 15 structures as their MFES. For each structure we sampled 10^4 sequences for our analyses of individual sequences and 200 more to use as initial sequences in our evolutionary simulations. We show in the section 4 of the Supplementary Text that using a different sampling method still yields qualitatively the same results.

Unless noted, results for all the 15 structures are very similar. Therefore, we present in the main text only results for sequences that have the structure of the CPEB3 ribozyme as their MFES. We report results for all other structures in the supplementary material.

Access to new phenotypes and robustness

To study the ensemble of secondary structures that a sequence s_i yields, we restricted ourselves to the analysis of the set of structures with a free energy in the interval of width D kcal mol^{-1} above the sequence's MFE, as in previous research [28; 29; 47–49]. We refer to such a set for s_i as the sequence's *plastic repertoire* Φ_i. We obtained these alternative structures using the ViennaRNA library [44], that applies Wuchty et al's algorithm [22] for this purpose. Unless noted, $D = 2$ kcal mol^{-1}, which is approximately equal to $3.2kT$ at the default temperature of 37 °C. We picked this value of D as a compromise between fast computation and finding a considerable number of the structures with non-negligible stability (Supplementary Table ST3).

The *mutational repertoire* Ξ_i of an L-nucleotide sequence s_i is the set of structures that are accessible to that sequence through single mutations. We obtained it by assaying separately the $3L$ possible nucleotide

substitutions and reviewing each mutant sequence's MFES. To evaluate the mutational access to a specific structure, we counted the number of single mutations that lead to a sequence with that structure as its MFES. A sequence may produce two or more structures with the same MFES. In such a situation, we added all the MFES to its mutational repertoire. In this case, we increased the mutational access to each of these structures by one over the number of MFES in that mutant sequence.

We evaluated a sequence's mutational robustness by assessing the fraction of all possible single mutations that produce the same structure as its MFES. We estimated the partition function Z_i associated to a sequence s_i as the sum of the Boltzmann factors of the structures in the plastic repertoire. Hence, we obtained the Boltzmann probability $p(\sigma_i^j) = B_{i,j}$ of the plastic repertoire's j-th structure σ_i^j dividing its Boltzmann factor by Z_i. We used the Boltzmann probability of a sequence's MFES as an indicator of its thermodynamic stability.

We assessed a sequence's intersection between its mutational and plastic repertoires, Ξ_i and Φ_i, using the overlap coefficient, that equals the cardinality of the intersection of two sets divided by the cardinality of the smaller set. We also used the Pearson correlation coefficient to evaluate the association between, on the one hand, mutational access to the structures in a sequence's mutational repertoire and, on the other hand, the thermodynamic stability of the structures in the sequence's plastic repertoire.

We evaluated whether the overlap, or the correlation, between Ξ_i and Φ_i were greater than as expected by chance. To do so, we performed paired analyses in which we compared, for each sequence s_i in our sample, the overlap, or correlation, between Ξ_i and Φ_i to the one between s_i's mutational repertoire and the plastic repertoire of another sequence s_j picked at random among those sequences that yield the same MFES as s_i.

Ancel-Fontana model

Ancel and Fontana considered that the fitness ω_i associated to a nucleotide sequence s_i equaled the sum of the contributions of the structures in its plastic repertoire Φ_i, i.e. the structures that such sequence could adopt [28]. The contribution of a structure σ_i^j to fitness depended both on its Boltzmann probability $p(\sigma_i^j) = B_{i,j}$, which is associated to its expected abundance in a cell, and on its resemblance $r(\sigma_i^j, \tau)$ to a pre-defined optimal structure τ. More specifically,

$$\omega_i = \sum_{\sigma_i^j \in \mathcal{P}_i} B_{i,j} r(\sigma_i^j, \tau), \tag{1}$$

where

$$r(\sigma_i^j, \tau) = \frac{1}{0.01 + d(\sigma_i^j, \tau)}. \tag{2}$$

$d(\sigma_i^j, \tau)$ measures the structural distance between structure σ_i^j and τ. Ancel and Fontana assessed the dissimilarity between two structures using the Hamming distance between the parenthetical notation for RNA secondary structures [28]. Here we instead assess how similar is the arrangement of loops and stacks in the two structures using the tree-edit distance [50], as implemented in the ViennaRNA library [44], but normalized with respect to the sequence's length.

RNA-ligand model

In this model we assume the existence of a molecular ligand with a constant concentration $\mathcal{L}_{i,T}$ in cell i. The cell's fitness depends on the equilibrium concentration of the complex that results from the binding of the cellular copies of an RNA molecule to such ligand. For simplicity and for the purpose of comparison with previous work [28], we consider that an RNA molecule's ability to bind the ligand only depends on its secondary structure. Thus we assume an optimal structure τ with maximum affinity for the ligand. An RNA sequence s_i may adopt any structure σ_i^j in its plastic repertoire Φ_i, a set with cardinality $M_i = |\Phi_i|$. We consider that $\mathcal{R}_{i,T}$, the total amount of copies of the RNA molecule in the cell, remains constant. For simplicity, we also assume that the population of free RNA molecules immediately attains thermodynamic equilibrium, in which the abundance of any such structural configuration will depend on the amount of free RNA molecules ($\sum_{j=1}^{M_i} R_{i,j}$) and the structure's Boltzmann probability $p(\sigma_i^j) = B_{i,j}$. This assumption is irrelevant when the whole system is at equilibrium. Namely, under equilibrium conditions, this model is indistinguishable from a more complicated version that explicitly includes transition rates between the different structural configurations in a sequence's plastic repertoire (section 1 of the Supplementary Text).

The dynamics of the system in a cell i with RNA sequence s_i are described by

$$\begin{aligned}
\frac{dC_{i,1}}{dt} &= k_+ B_{i,1}(\mathcal{R}_{i,T} - \sum_{j=1}^{M_i} C_{i,j})(\mathcal{L}_{i,T} - \sum_{j=1}^{M_i} C_{i,j}) - k_{-,i,1} C_{i,1} \\
&\vdots \qquad\qquad\qquad \vdots \\
\frac{dC_{i,m}}{dt} &= k_+ B_{i,m}(\mathcal{R}_{i,T} - \sum_{j=1}^{M_i} C_{i,j})(\mathcal{L}_{i,T} - \sum_{j=1}^{M_i} C_{i,j}) - k_{-,i,m} C_{i,m} \\
&\vdots \qquad\qquad\qquad \vdots \\
\frac{dC_{i,M_i}}{dt} &= k_+ B_{i,M_i}(\mathcal{R}_{i,T} - \sum_{j=1}^{M_i} C_{i,j})(\mathcal{L}_{i,T} - \sum_{j=1}^{M_i} C_{i,j}) - k_{-,i,M_i} C_{i,M_i}
\end{aligned} \tag{3}$$

, where $C_{i,m}$ denotes the amount of complex of structure σ_i^m and ligand, $B_m(\mathcal{R}_{i,T} - \sum_{j=1}^{M_i} C_{i,j})$ is the amount of free RNA with structure σ_i^m, $(\mathcal{L}_{i,T} - \sum_{j=1}^{M_i} C_{i,j})$ is the amount of non-bound ligand. k_+ is the association constant that we consider the same for all alternative structures. In this model, an RNA molecule's structure only affects the dissociation rate of their complex with the ligand. This assumption is pertinent not only because it allows a simpler analysis; despite noteworthy exceptions, related molecules that bind the same ligand frequently differ much more on their dissociation rates than on their association rates [51–53]. In the model, the dissociation constant $k_{-,i,j}$ for complex $C_{i,j}$ increases with the structural distance between structure σ_i^j and the optimal structure τ according to

$$k_{-,i,j} = \alpha 2^{\beta d(\sigma_i^j, \tau)}. \tag{4}$$

Equations in system (3) are quadratic on several variables. Although there is no general method to solve such systems, we identified properties that allowed us to solve this system exactly (section 2 in Supplementary Text). Moreover, we used previous results on rank-one perturbations of diagonal matrices [54] to show that the system (3) has a unique stable equilibrium point under physically meaningful conditions (section 2 in Supplementary Text). Unless noted, parameter values are $\mathcal{R}_{i,T} = 20$ nM, $k_+ = 0.001$ nM^{-1}s^{-1}, $\alpha = 0.001$s^{-1}, $\beta = 0.5$.

Evolutionary simulations

We started a population with N identical copies of a nucleotide sequence picked at random among those with the ability to fold into a target secondary structure τ as their MFES. Then, we submitted the population

to cycles, i.e. generations, of mutation and selection.

Regarding mutation, for each sequence of length L we obtained an integer $0 \leq u \leq L$ from a binomial distribution $\text{Bin}(L, \mu)$, where μ is the per-nucleotide mutation rate. Then we picked at random u nucleotides from the sequence and replaced them at random. We obtained a sequence's fitness depending on the model that we followed: Ancel-Fontana, or RNA-ligand, as described above. In all cases, structures more similar to τ conferred a greater selective advantage; that is, the populations evolved under stabilizing selection. Next, we applied fitness proportional selection to sample with replacement N individuals that constitute the next generation. We repeated these steps for G generations.

We analyzed the simulation results using a two-way mixed ANOVA for each of the independent variables that we assessed. We used the optimal structure and scenario as factors, with repeated measures for populations evolving from the same ancestral sequence under different scenarios. For post-hoc tests, we corrected for multiple hypothesis testing using false discovery rate [55]. Our default parameter values are: $N = 10^3$, $\mu = 5 \times 10^{-5}$, $G = 3 \times 10^4$.

Results

Sequestration of molecules with optimal structures in the RNA-ligand model

To test the validity of our RNA-ligand scenario, we first studied hypothetical RNA molecules that we assume only fold into two structures: an optimal structure τ and a non-optimal structure υ at a fixed structural distance d from τ. Because we expected that the behavior of the system varied with the amount of ligand respective to the amount of RNA, we assayed three different concentrations of ligand molecule. We also studied these hypothetical RNA molecules under the perspective of the Ancel-Fontana model. For the Ancel-Fontana model [28] we measured fitness as the average contribution to fitness of each structure, weighted by each structure's thermodynamic stability (see details in Methods). In the RNA-ligand model, we quantified fitness as the total amount of RNA-ligand complex at thermodynamic equilibrium. In all scenarios, the theoretical maximum fitness value corresponds to a sequence with a plastic repertoire that only contains the optimal structure. We use such maximum fitness as a normalization constant thus allowing us to compare relative fitness fairly among different scenarios.

Fig. 1 shows fitness (blue line) as a function of the thermodynamic stability of the optimal structure. The figure shows that fitness increases linearly with the stability of the optimal structure τ in the Ancel-Fontana model. In the RNA-ligand model, fitness also increases monotonically with τ's stability. However, in this

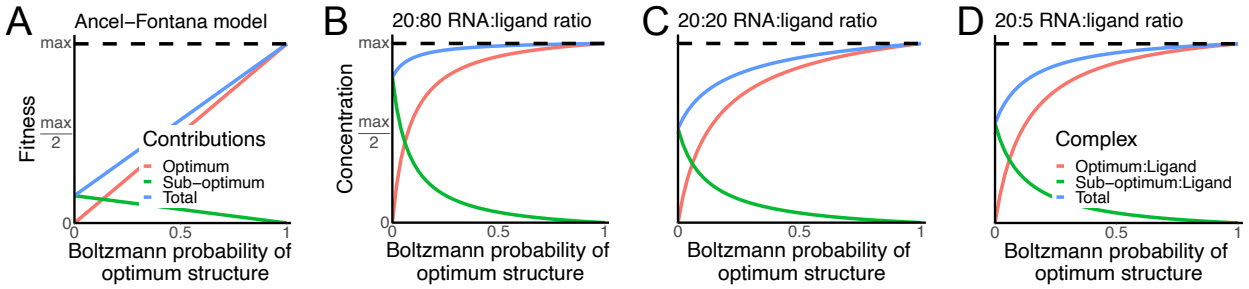

Fig. 1. Fitness as a function of thermodynamic stability of a sequence's MFES. We assume that all sequences have two different structures in their plastic repertoire: an optimal structure τ and a second structure υ at a fixed structural distance $d = 8$ from τ. Green and red lines indicate υ's and τ's contribution to fitness, respectively. The blue line refers to the sequence's total fitness. The horizontal dashed line indicates the maximum fitness value in each scenario.

case fitness is a concave function of B_i: as the Boltzmann probability increases, further increase leads to a slighter fitness gain. As we expected, concavity, relative fitness and, consequently, selective proximity to the optimum, are the greatest when the ligand concentration is the highest; in this case the excess molecules of ligand are able to sequester a greater amount of RNA molecules with the optimal structure. For the examples in Fig. 1 we maintained a fixed, relatively low, structural distance $d = 8$ between the optimal structure τ and the suboptimal structure. Fig. SF1 in Supplementary Figures shows that the effect is qualitatively the same even when we fix a much higher value for d.

Fitness as a concave function of thermodynamic stability in the RNA-ligand model

For Fig. 1 we applied our RNA-ligand model to simplified hypothetical RNA molecules that, non-realistically, always have the same two structures in their plastic repertoires. Now we do the same but for RNA sequences, first, that can fold into complex and diverse ensembles of structures defined by RNA biophysics and, second, in which we have described the association between variation produced by mutation and thermal fluctuations, as shown in section 3 of the Supplementary Text. For comparison, we also study the influence of thermodynamic stability on fitness in the Ancel-Fontana model.

Notwithstanding the intricacies of RNA folding into ensembles of secondary structures, our results are very similar to the ones that we presented for hypothetical simplified RNA molecules. Fig. 2 shows our results for sequences that fold into the structure of the CPEB3 ribozyme as their MFES. The corresponding data for the remaining structures in our study, biological or random, appear in Supplementary Figures SF2,3, respectively. We confirmed that the relationship between the Boltzmann probability of the MFES and fitness is near-linear in the Ancel-Fontana model: mutations that increase thermodynamic stability to the same

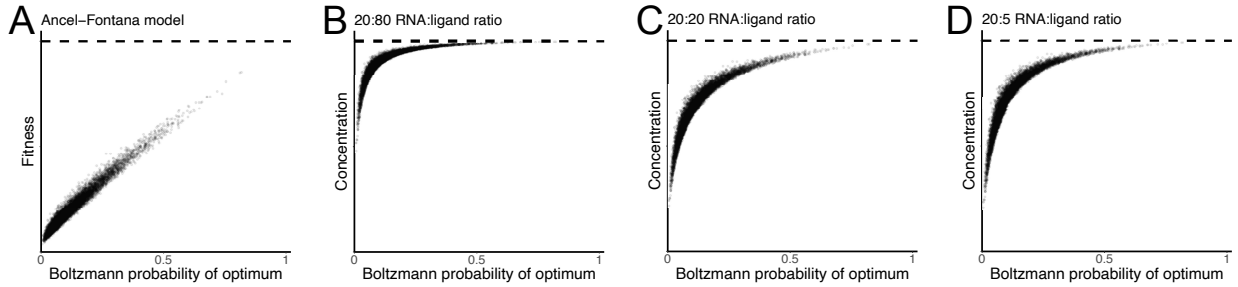

Fig. 2. Fitness as a function of thermodynamic stability in sequences that fold into the structure of the CPEB3 ribozyme as their MFES. We assess thermodynamic stability as a sequence's Boltzmann probability for the structure of the CPEB3 ribozyme. The horizontal dashed line indicates the maximum fitness value in each scenario.

extent would always produce the same increment in fitness. In contrast, in our RNA-ligand model and according to our expectations, fitness is a concave down function of thermodynamic stability. Hence, adding to a sequence a series of mutations that increase more and more the Boltzmann probability of a structure with a high affinity for the ligand would result in diminishing fitness returns.

Our hypothesis states that sequestration of optimal and near-optimal structures in RNA-ligand complexes creates a net conversion of unbound molecules to high-affinity structures, replenishing their stock. In this scenario, even with a lower stability, the sequestration-driven accumulation of high-affinity structures would increase complex formation. Thus, we expect that a high concentration of ligand would increase relative fitness and hence its selective proximity to the optimum. It would also intensify fitness concavity as a function of thermodynamic stability. After all, the sequestration of near-optimal of structures would be stronger when there are more ligand molecules. Fig. 2 and Supplementary Figures SF2,3 show that relative fitness and its concavity are indeed greatest in the simulations in which we considered the highest ligand concentration. This is more evident in Fig. 3 and Supplementary Figures SF4,5, that show that a sequence's relative fitness is always the greatest, and hence more proximate to the maximum, in the ligand-RNA model under high ligand concentrations. The figures also show that relative fitness is always the lowest, farther from the maximum value, under the Ancel-Fontana model. However, the story is not straightforward: concavity and relative fitness do not decrease monotonically as the ligand concentration diminishes. The plots of fitness as a function of thermodynamic stability for intermediate and low concentrations of ligand (Fig. 2 and Supplementary Figures SF2 and SF3) seem very similar. However, the pattern is clearer in the direct comparison of relative fitness between these two models: Relative fitness is slightly but always higher for low than for intermediate concentrations of ligand (Fig. 3 and Supplementary Figures SF4,5). In fact, we

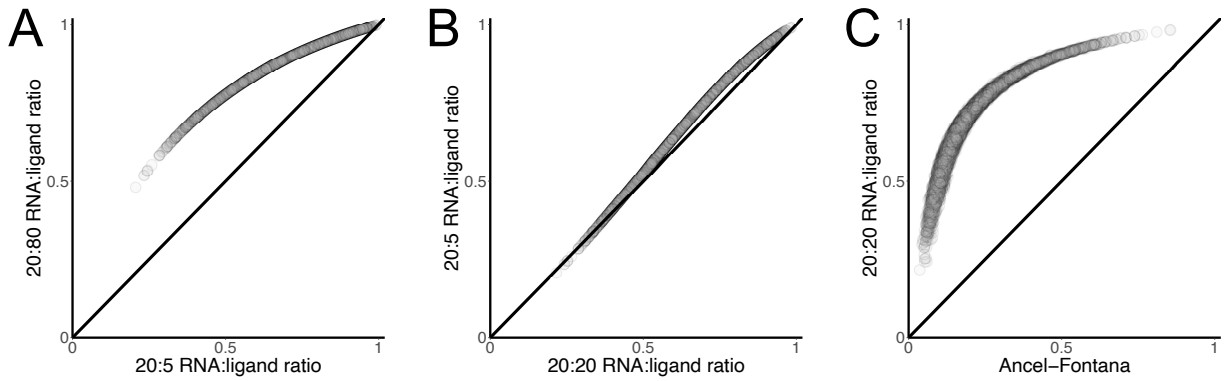

Fig. 3. Comparison of relative fitness under different models or ligand concentrations for sequences that fold into the structure of the CPEB3 ribozyme. In all panels, the diagonal indicates the identity line. Points above the diagonal refer to sequences with a higher fitness under the model/ligand concentration that corresponds to the vertical axis than under conditions described in the horizontal axis. Fitness values are normalized with respect to the maximum fitness value for the respective model.

also observed this pattern when we studied the hypothetical simplified RNA molecules for Fig. 1. All these observations suggest that ligand binding implies an additional effect, stronger at low ligand concentrations, that increases relative fitness.

Additional effects of RNA-ligand binding on relative fitness

One of the additional effects that we expect is that RNA molecules saturate ligand molecules more easily when the latter are scarce, requiring less RNA molecules with a high ligand-affinity structure to approach the maximum amount of RNA-ligand complex. To observe and better study this effect, we developed a new version of our model in which, as a non-realistic and non-natural experiment, we blocked transitions in free RNA molecules from one structure in the plastic repertoire to another, preventing the sequestration-dependent flux towards structures with higher affinity for the ligand. Namely, we consider that the number of RNA molecules that fold into a certain structure υ, whether free or ligand-bound, remains constant and proportional to υ's Boltzmann probability. The m-th of M equations that describe this version of the model is

$$\frac{dC_{i,m}}{dt} = k_+(B_{i,m}\mathcal{R}_{i,T} - C_{i,m})(\mathcal{L}_{i,T} - \sum_{j=1}^{M_i} C_{i,j}) - k_{-,i,m}C_{i,m} \tag{5}$$

. The term $(B_{i,m}\mathcal{R}_{i,T} - C_{i,m})$ defines the abundance of free RNA molecules with structure σ_i^m. It equals the total amount of RNA molecules with that structure, held constant at a value of $B_{i,m}\mathcal{R}_{i,T}$, minus the portion of those molecules that take parte in RNA-ligand complexes. We used Powell's hybrid method [56; 57] as implemented in the GSL library [58] to assess the complex concentration at equilibrium.

This version of the model shows much more dispersion on fitness values, suggesting that particularities of each sequence s_i and of its plastic repertoire Φ_i play a more important role in it (Supplementary Figures SF6,7). Supporting that RNA-ligand complexes saturate more easily at low ligand concentrations, we found that, when we prohibit transitions between alternative RNA structures, concavity and relative fitness are greatest in the scenario in which ligand concentration is lowest (Supplementary Figures SF6-9). However, the association between ligand abundance and relative fitness is neither monotonic in this case; relative fitness and, consequently, proximity to the optimum, are slightly greater under high than under intermediate ligand concentrations (Supplementary Figures SF8,9), suggesting that there is a third additional factor that increases relative fitness at high ligand concentrations. The effect is clearer at low Boltzmann probabilities for the optimal structure (Supplementary Figures SF6,7). We hypothesized that this effect occurred because, when ligand is in excess, molecules with a lower affinity structure can also bind the ligand, increasing the concentration of RNA-ligand complex. We reasoned that this effect should be sensitive to the affinity for the ligand of molecules in the plastic repertoire: a very low affinity would hinder it severely. Testing this hypothesis with sequences that fold into large and diverse ensembles of structures following intricate patterns dictated by RNA biophysics would be complicated. We then studied the version of the model in which we block transitions between different structures but now applying it to hypothetical simplified RNA molecules with only two structures in their plastic repertoire. Consistently with our hypothesis, when ligand is in excess, molecules with a lower affinity structure can also bind the ligand, increasing the concentration of RNA-ligand complex. However, if the affinity is too small, ligand abundance is not sufficient to recruit RNA molecules into complexes (Supplementary Figure SF10).

Attenuation of neutral confinement in evolution under stabilizing selection

We have shown that explicitly considering the binding of RNA molecules to a ligand to form functional complexes reveals fitness as a concave down function of thermodynamic stability in which the relative fitness difference to the optimum is diminished. We designed evolutionary simulations to assess whether weakening the selective incentive to increase thermodynamic stability obstructs the appearance of neutral confinement. We compared populations evolving in either the Ancel-Fontana scenario, under which neutral confinement easily evolves [28], or in the RNA-ligand scenario, with three different levels of ligand abundance. We expected neutral confinement to be strongest in the Ancel-Fontana scenario; within the RNA-ligand scenario, our previous results suggest that neutral confinement would decrease its strength from intermediate to low

and high concentrations of ligand. Our simulations occur in a stabilizing selection regime: evolution starts with sequences that already produce the optimum structure as their MFES, although not necessarily with a high thermodynamic stability. We designed our simulations this way to avoid complications in our analysis and to focus on a population's accumulation of genetic variation and its ability to access different phenotypes. We picked one of the structures in Supplementary Tables ST1 and ST2 as the optimal structure for each of our simulations. In the Ancel-Fontana model, stabilizing selection favors those sequences that yield a stabler optimal structure. In the RNA-ligand models the optimal structure has the highest affinity for the ligand and stabilizing selection favors sequences that produce a higher RNA-ligand complex equilibrium concentration. The results of the statistical analyses of these simulations appear complete in Supplementary Tables ST4-33 and Supplementary Figs. SF11-20.

First we compared the amount of genetic variation that populations hold after 3×10^4 generations of evolution under stabilizing selection. We found that the scenario has a significant effect on the amount of genetic variation that populations hold and that this observation is valid regardless the identity of the optimal structure (Supplementary Tables ST4,5). Moreover, as expected, the number of different sequences in the population is, in all cases, significantly lowest in the Ancel-Fontana scenario and significantly highest in the high-ligand RNA-ligand setup (Fig. 4A, Supplementary Table ST6, Supplementary Fig. SF11). We also considered other measures of genetic diversity like heterozygosity, nucleotide diversity [59; 60] and the maximum number of nucleotide differences between any two sequences in the population. They follow the same pattern; however, the results of the post-hoc tests for these other indicators of genetic variation are not as consistent as for the number of different sequences in the population (Supplementary Tables ST7-15 and Supplementary Figs. SF12-14).

As expected, thermodynamic stability (Fig. 4B, Supplementary Tables ST16-18 and Supplementary Fig. SF15) and mutational robustness (Supplementary Fig. SF16, Supplementary Table ST19-21) follow a similar pattern, opposite to that of genetic variation. Despite their similar trend, average differences are much more pronounced in the case of thermodynamic stability. Together, these findings support that the RNA-ligand scenario tends to diminish the concentration of individuals with high robustness genotypes.

In addition, we looked at the access to new secondary structures. Access to new structures through plasticity, as indicated by the size of a sequence's plastic repertoire, was significantly higher in sequences evolved under the RNA-ligand scenario than in those evolved in the Ancel-Fontana scenario (Fig. 4C, Supplementary Fig. SF17, Supplementary Tables ST22-24). In contrast, a sequence's average mutational repertoire was not

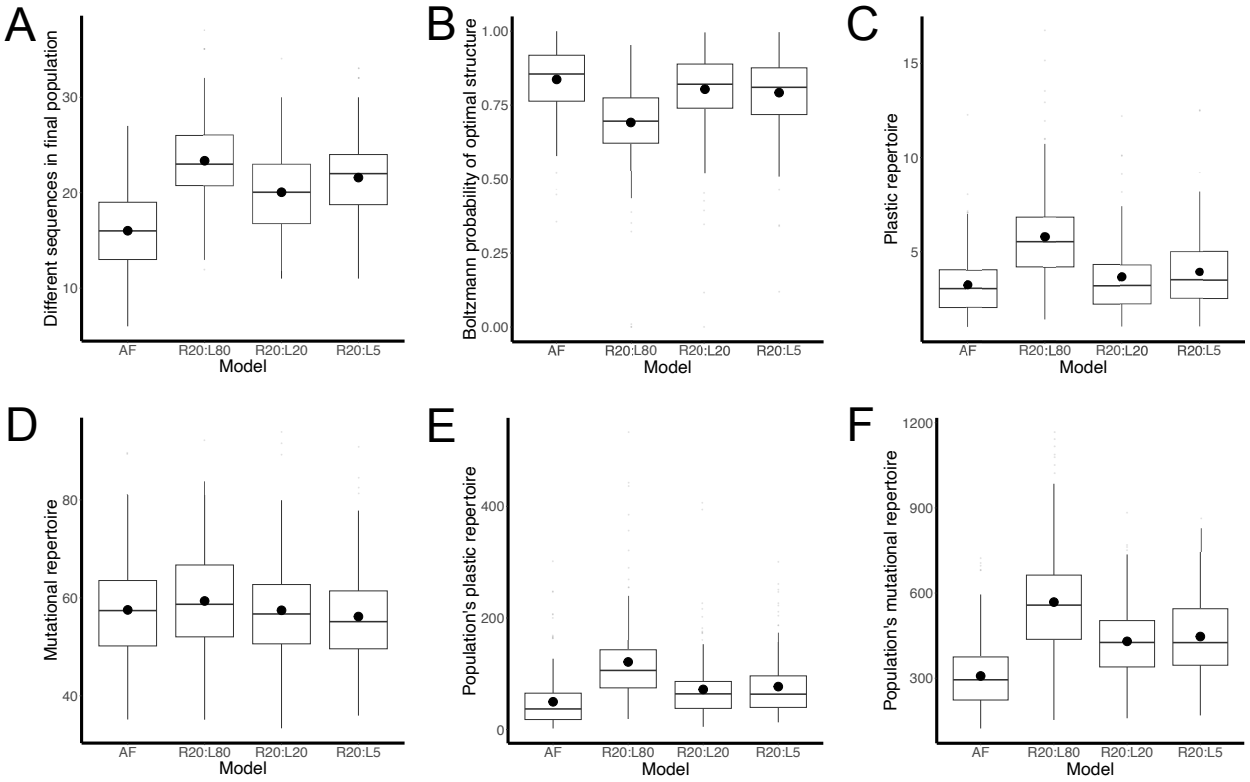

Fig. 4. Evolution under stabilizing selection in favor of the CPEB3 ribozyme structure under different scenarios. AF: Ancel-Fontana model; RX:LY: RNA-ligand scenario with X and Y as the constant concentrations of the RNA molecule and the ligand, respectively. A. Number of distinct sequences in the population at the end of evolution. B. Average thermodynamic stability at the end of evolution. C,D. Cardinality of the plastic and mutational repertoires, respectively. E,F. Population's access to new phenotypes through plasticity and mutation, respectively. We define the population's plastic, or mutational, repertoire as the union of the plastic, or mutational, repertoires of all the sequences that comprise a population.

always significantly lower in the Ancel-Fontana than in the RNA-ligand scenario (Fig. 4D, Supplementary Tables ST25-27, Supplementary Fig. SF18). Indeed, for several optimal structures we failed to find a significant effect of the model on the size of the mutational repertoire of individual sequences (Supplementary Table ST26). For example, sequences folding into the structure of the CPEB3 ribozyme that evolved under selection for complex formation have mutational repertoires without significant differences to those of sequences evolved in the Ancel-Fontana scenario (Fig. 4D, Supplementary Table ST27).

While individual sequences evolved under the RNA-ligand scenario do not have easier mutational access to new structures, there may still be differences in the mutational access to new structures at the level of the population. The increased genetic variation in populations that evolved under the RNA-ligand scenario might imply a smaller overlap between the mutational (or plastic) repertoires of different sequences of the

population. If this were the case, a more diverse population may have access to a wider range of structural diversity, despite similar access to new structures of individual sequences. To assess this possibility we define a population's plastic repertoire as the union of all the plastic repertoires of the sequences that comprise a population; it lists all the structures that appear in the plastic repertoire of at least one of the population's individuals. Analogously, we define the population's mutational repertoire as the union of the mutational repertoires of all the population's individuals.

We found that a population's access to new structures through either mutation or plasticity is clearly greater in populations that evolved under the RNA-ligand scenario (Figs. 4E,F, Supplementary Tables ST28-33 and Supplementary Figs. SF19,20). For example, populations that evolved in the Ancel-Fontana scenario under selection for the structure of the CPEB3 ribozyme could access, on average, 307.9 structures through mutation and 49.8 through plasticity. In contrast, when they evolved in the RNA-ligand scenario under high-ligand conditions, populations could access 568.1 and 121.2 through mutation and plasticity, respectively. Even under conditions of intermediate ligand concentrations, the worst case among the RNA-ligand scenarios, there is much easier access to new structural variation (429.9 through mutation and 71.96 through plasticity) than in populations evolved in the Ancel-Fontana setup (Figs. 4E,F; Supplementary Tables ST30,33). Populations that evolved under selection for any of the structures that we studied clearly follow the same pattern (Supplementary Tables ST28-33 and Supplementary Figs. SF19,20).

Discussion

Previous research has established that a consistent increase in the stability of one RNA structure υ at the expense of others leads to neutral confinement. A population in neutral confinement becomes locked in a cluster of sequences that produce a highly stable υ configuration but with scant mutational access to new, perhaps better, structures [23; 28; 29; 34; 61]. One could say that sequences become victims of their success. The support to the idea of neutral confinement rests on three sound and robust premises: first, RNA structure as a strong determinant of biological function [5–11; 13–17]; second, within-cell conformational diversity of the structures of RNA molecules with the same sequence [7; 17–21]; and third, plastogenetic congruence, a positive association between the amount and kind of structural variation produced by thermal fluctuations and mutation [22; 29–33, section 3 of Supplementary Text]. Nevertheless, although all three premises hold, the consequences of neutral confinement are not apparent in nature, as indicated by the diversity of molecular functions that RNA molecules have acquired in all lineages throughout evolution [4]. One way in which RNA

molecules may escape neutral confinement is through recombination of different sequences [28; 29; 34]. Ultimately, recombination can merge in one sequence different substructures with independent evolutionary histories. The creation of innovation through recombination in RNA sequences seems to be frequent in RNA viruses [35; 36] and probably was also important during the RNA world [37]. However, to our knowledge, there is no evidence that supports it as a common evolutionary mechanism for RNA structural innovation in modern cellular organisms.

Here we put forward an alternative to avoid neutral confinement in the evolution of RNA. Our alternative does not dispute any of the three important premises that uphold neutral confinement. In our proposal, the function of an RNA molecule depends on specific binding to a ligand to form an RNA-ligand complex and affinity for the ligand depends on the RNA's structure. Our work identifies three important effects of ligand binding:

- Ligand molecules may function as sinks for RNA molecules with a configuration with higher affinities for the ligand, that they easily entrap into RNA-ligand complexes. As the free RNA molecules wiggle because of thermal fluctuations, they replenish the stock of molecules with a high affinity structure.
- Under low ligand concentrations, most ligand molecules bind high-affinity RNA molecules promptly. Since most ligand molecules are occupied, availability of additional high-affinity RNA molecules produces only marginal increases in the amount of RNA-ligand complex.
- Under high ligand concentrations not only high-affinity molecules bind the ligand; but a significant fraction of RNA molecules with alternative configurations also can bind the abundant free ligand molecules.

Assuming that organismal fitness depends on the amount of RNA-ligand complex, all these factors diminish the fitness difference between organisms with an RNA sequence that produce the same structure but with different Boltzmann probabilities. Thus, populations lack a strong incentive to evolve sequences that produce extraordinarily stable structures but with a meager mutational access to new structures. As our simulations of evolution show, instead of neutral confinement, populations may retain genetic variation within a population, preserve access to new structures through mutation and thermal fluctuations, and maintain the ability to explore genotype space through nearly-neutral mutations.

In our model, the most important way in which ligand-binding weakens neutral confinement is by the sequestration into complexes of high affinity configurations and the consequent restoration of their supply

by thermal fluctuations. Outside of the context of RNA evolution, the idea that binding to a ligand can shift the equilibrium distribution of protein conformations is not novel and is well studied [62–64]. For example, *ligand-directed conformational selection* is one of the central ingredients in the Monod-Wyman-Changeux model for allosteric regulation [65–67]. Otherwise, our model hinges on the three same premises for neutral confinement and the reasonable consideration that much of RNA's function depends on binding to other molecules to form multimeric complexes [4]. Thus, it may be relevant and valid for a wide range of cases.

Our evolutionary simulations revealed that accumulation of genetic variation is critical for facilitating mutational access to new structures. Indeed, we were unable to find consistent significant increases in the size of the mutational repertoires of individual sequences that evolved in our RNA-ligand scenario. However, once we look at the ability to yield new structures after mutation in the whole population, a clear pattern was evident: the more diverse set of sequences allowed the whole population an easier access to new RNA secondary structures. The reason is that the mutational repertoires of more diverse sequences tend to be more different [68]. It is noteworthy that a higher access to new structures through plasticity in the RNA-ligand scenario does not require accruing genetic variation; individual sequences that evolved in such scenario typically yield a more diverse plastic repertoire. This observation is important because, as our work shows, non-MFE structures are not negligible: they may increase their abundance if they have a high affinity for a ligand. Therefore, the enhanced diversity in individual plastic repertoires may be relevant for the discovery of new functional structures. Regardless, our work also shows that a population's access through plasticity to new structures also benefits from increased genetic variation (Figs. 4F). This occurs because, as reported previously, a few substitutions can significantly alter a sequence's plastic repertoire [49].

In this contribution we focused on whether considering ligand-binding explicitly was sufficient to undermine neutral confinement. In our evolutionary simulations, populations evolved in a stabilizing selection regime: the optimal RNA structure was present in the population as a minimum free energy structure from the beginning of our simulations, although perhaps not with a very high thermodynamic stability. Further research is necessary to evaluate how our scenario, and the consequent erosion of neutral confinement, impacts on the evolution of novel structures. Indeed there are interesting observations that suggest that formation of functional RNA-ligand complexes can accelerate evolution of new structures in the face of RNA conformational diversity. First, previous research already shows that a few mutations can change many of the structures in a plastic repertoire [49]. Hence, exploration of those structures accessible through thermal fluctuations may allow faster discovery of structures with enhanced functionality, albeit most often with a low

thermodynamic stability. Importantly, our work supports that a structure with high propensity to assemble complexes but with a low thermodynamic stability can confer a non-negligible fitness benefit, facilitating the action of selection. In this case, the few molecules with the new functional structure would form a complex promptly, promoting the conversion of other molecules into the high affinity configuration. Moreover, once a population is enriched with sequences with the high affinity structure in their plastic repertoire, plastogenetic congruence may favor the appearance of sequences that produce the beneficial structure with higher stability or even as their MFES. The existence of clusters of similar sequences that can access the same structure through mutations [69] could facilitate further these transitions. Validation of this prospect by future research would strengthen the case of plasticity in RNA secondary structures as an evolutionary asset instead of an obstacle, as in other kinds of biological systems, including protein structure [27], gene expression patterns [70–72] and morphology [73–75].

Supplementary material

Supplementary Text, Tables and Figures are available online.

Acknowledgements

We thank the most valuable technical assistance from JC Sánchez-Leaños and useful comments by L.F. Meraz-Segura, A.G. Cruz-Moreno and H.J. Villasana.

Authors' contributions

AL and CE-S developed code and performed research. CE-S, AL, and EU developed the differential equation model, analyzed the data and designed research. CE-S wrote the paper. All authors revised and approved the paper.

References

[1] Higgs PG, Lehman N. The RNA World: Molecular cooperation at the origins of life. Nat Rev Genet. 2015;16:7–17.

[2] Vázquez-Salazar A, Lazcano A. Early Life: Embracing the RNA World. Curr Biol. 2018;28:R208–R231.

[3] Briggs JA, Wolvetang EJ, Mattick JS, Rinn JL, Barry G. Mechanisms of long non-coding RNAs in mammalian nervous system development, plasticity, disease, and evolution. Neuron. 2015;88:861–877.

[4] Mattick J, Amaral P. RNA. The epicenter of genetic information. Boca Raton, Fl: CRC Press, Taylor and Francis Group; 2023.

[5] Kieft JS, Zhou K, Jubin R, Murray MG, Lau JYN, Doudna JA. The hepatitis C virus internal ribosome entry site adopts an ion-dependent tertiary fold. J Mol Biol. 1999;292:513–529.

[6] Varani G. RNA structure. In: Encyclopedia of Life Sciences. Chichester, UK: John Wiley and Sons; 2001. p. 18.

[7] Dethoff EA, Chugh J, Mustoe AM, Al-Hashimi HM. Functional complexity and regulation through RNA dynamics. Nature. 2012;482:322–330.

[8] Chen YJ, Liu P, Nielsen AAK, Brophy JAN, Clancy K, Peterson T, et al. Characterization of 582 natural and synthetic terminators and quantification of their design constraints. Nat Methods. 2013;10:659–664.

[9] Ritz J, Martin JS, Laederach A. Evolutionary evidence for alternative structure in RNA sequence co-variation. PLoS Comput Biol. 2013;9:e1003152.

[10] Wan Y, Qu K, Zhang QC, Flynn RA, Manor O, Ouyang Z, et al. Landscape and variation of RNA secondary structure across the human transcriptome. Nature. 2014;505:706–709.

[11] Hudson AJ, Wieden Hj. Rapid generation of sequence-diverse terminator libraries and their parameterization using quantitative. Synth Biol. 2019;4:ysz026.

[12] Dingle K, Ghaddar F, Šulc P, Louis AA. Phenotype bias determines how natural RNA structures occupy the morphospace of all possible shapes. Mol Biol Evol. 2022;39:msab280.

[13] Lin J, Chen Y, Zhang Y, Lin H, Ouyang Z. Deciphering the role of RNA structure in translation efficiency. BMC Bioinformatics. 2022;23:559.

[14] Zhang J, Fei Y, Sun L, Zhang QC. Advances and opportunities in RNA structure experimental determination and computational modeling. Nat Methods. 2022;19:1193–1207.

[15] Klapproth C, Zötzsche S, Kühnl F, Fallmann J, Stadler PF, Findeiß S. Tailored machine learning models for functional RNA detection in genome-wide screens. NAR Genomics Bioinformatics. 2023;5:lqad072.

[16] Ken ML, Roy R, Geng A, Ganser LR, Manghrani A, Cullen BR, et al. RNA conformational propensities determine cellular activity. Nature. 2023;617:835–841.

[17] Lee YT. Nexus between RNA conformational dynamics and functional versatility. Curr Opin Struct Biol. 2024;89:102942.

[18] Rouskin S, Zubradt M, Washietl S, Kellis M, Weissman JS. Genome-wide probing of RNA structure reveals active unfolding of mRNA structures in vivo. Nature. 2014;505:701–705.

[19] Woods CT, Lackey L, Williams B, Dokholyan NV, Gotz D, Laederach A. Comparative visualization of the RNA suboptimal conformational ensemble in vivo. Biophys J. 2017;113:290–301.

[20] Ganser LR, Kelly ML, Herschlag D, Al-Hashimi HM. The roles of structural dynamics in the cellular functions of RNAs. Nat Rev Mol Cell Biol. 2019;20:474–489.

[21] Bonilla SL, Jones AN, Incarnato D. Structural and biophysical dissection of RNA conformational ensembles. Curr Opin Struct Biol. 2024;88:102908.

[22] Wuchty S, Fontana W, Hofacker IL, Schuster P. Complete suboptimal folding of RNA and the stability of secondary structures. Biopolymers. 1999;49:145–165.

[23] Fontana W. Modelling 'evo-devo' with RNA. BioEssays. 2002;24:1164–77.

[24] Schultes EA, Bartel DP. One sequence, two ribozymes: implications for the emergence of new ribozyme folds. Science. 2000;289:448–452.

[25] James LC, Tawfik DS. Conformational diversity and protein evolution - A 60-year-old hypothesis revisited. Trends Biochem Sci. 2003;28:361–368.

[26] Tokuriki N, Tawfik DS. Protein dynamism and evolvability. Science. 2009;324:203–207.

[27] Khersonsky O, Tawfik DS. Enzyme promiscuity: a mechanistic and evolutionary perspective. Annu Rev Biochem. 2010;79:471–505.

[28] Ancel LW, Fontana W. Plasticity, evolvability, and modularity in RNA. J Exp Zool. 2000;288:242–283.

[29] Meyers LA, Lee JF, Cowperthwaite M, Ellington AD. The robustness of naturally and artificially selected nucleic acid secondary structures. J Mol Evol. 2004;58:681–691.

[30] Derényi I, Szöllosi GJ. Effective temperature of mutations. Phys Rev Lett. 2015;114:058101.

[31] Rezazadegan R, Reidys C. Degeneracy and genetic assimilation in RNA evolution. BMC Bioinformatics. 2018;19:543.

[32] Martin NS, Ahnert SE. Insertions and deletions in the RNA sequence-structure map. J R Soc Interface. 2021;18:20210380.

[33] Martin NS, Ahnert SE. The Boltzmann distributions of molecular structures predict likely changes through random mutations. Biophys J. 2023;122:4467–4475.

[34] Meyers LA, Fontana W. Evolutionary lock-in and the origin of modularity in RNA structure. In: Callebaut W, Rasskin-Gutman D, editors. Modularity: Understanding the development and evolution of natural complex systems. Cambridge, MA: MIT Press; 2005. p. 129–141.

[35] Simon-Loriere E, Holmes EC. Why do RNA viruses recombine? Nat Rev Microbiol. 2011;9:617–626.

[36] Sztuba-Solińska J, Urbanowicz A, Figlerowicz M, Bujarski JJ. RNA-RNA recombination in plant virus replication and evolution. Annu Rev Phytopathol. 2011;49:415–443.

[37] Manrubia SC, Briones C. Modular evolution and increase of functional complexity in replicating RNA molecules. RNA. 2007;13:97–107.

[38] Fontana W, Konings DAM, Stadler PF, Schuster P. Statistics of RNA secondary structures. Biopolymers. 1993;33:1389–1404.

[39] Schuster P. Genotypes and phenotypes in the evolution of molecules. In: Caetano-Anollés G, editor. Evolutionary genomics and systems biology. Hoboken, NJ: Wiley-Blackwell; 2010. p. 123–149.

[40] Schuster P, Fontana W. Chance and necessity in evolution: Lessons from RNA. Phys D Nonlinear Phenom. 1999;133:427–452.

[41] Flamm C, Hofacker IL, Maurer-Stroh S, Stadler PF, Zehl M. Design of multistable RNA molecules. RNA. 2001;7:254–265.

[42] Zuker M, Stiegler P. Optimal computer folding of large RNA sequences using thermodynamics and auxiliary information. Nucleic Acids Res. 1981;9:133–148.

[43] Turner DH, Sugimoto N, Freier SM. RNA structure prediction. Annu Rev Biophys Biophys Chem. 1988;17:167–192.

[44] Lorenz R, Bernhart SH, Höner Zu Siederdissen C, Tafer H, Flamm C, Stadler PF, et al. ViennaRNA Package 2.0. Algorithms Mol Biol. 2011;6:26.

[45] RNAcentral Consortium. RNAcentral 2021: Secondary structure integration, improved sequence search and new member databases. Nucleic Acids Res. 2021;49:D212–D220.

[46] Hofacker IL, Fontana W, Stadler PF, Bonhoeffer S, Tacker M, Schuster P. Fast folding and comparison of RNA secondary structures. Monatshefte für Chemie Chem Mon. 1994;125:167–188.

[47] Cowperthwaite MC, Bull JJ, Meyers LA. Distributions of beneficial fitness effects in RNA. Genetics. 2005;170:1449–1457.

[48] Szöllosi GJ, Derényi I. Congruent evolution of genetic and environmental robustness in micro-RNA. Mol Biol Evol. 2009;26:867–874.

[49] Wagner A. Mutational robustness accelerates the origin of novel RNA phenotypes through phenotypic plasticity. Biophys J. 2014;106:955–965.

[50] Shapiro BA, Zhang K. Comparing multiple RNA secondary structures using tree comparisons. Cabios. 1990;6:309–318.

[51] Tummino PJ, Copeland RA. Residence time of receptor-ligand complexes and its effect on biological function. Biochemistry. 2008;47:5481–5492.

[52] Núñez S, Venhorst J, Kruse CG. Target-drug interactions: First principles and their application to drug discovery. Drug Discov Today. 2012;17:10–22.

[53] Sykes DA, Stoddart LA, Kilpatrick LE, Hill SJ. Binding kinetics of ligands acting at GPCRs. Mol Cell Endocrinol. 2019;485:9–19.

[54] Ionascu EJ. Rank-one perturbations of diagonal operators. Integr Equations Oper Theory. 2001;39:421–440.

[55] Benjamini Y, Hochberg Y. Controlling the false discovery rate: a practical and powerful approach to multiple testing. J R Stat Soc B. 1995;57:289–300.

[56] Powell MJD. A hybrid method for nonlinear equations. In: Rabinowitz P, editor. Numer. methods nonlinear Algebr. equations. London, UK: Gordon and Breach Science Publishers; 1970. p. 87–114.

[57] Powell MJD. A Fortran subroutine for solving systems of nonlinear algebraic equations. In: Rabinowitz P, editor. Numer. methods nonlinear Algebr. equations. London, UK: Gordon and Breach Science Publishers; 1970. p. 115–162.

[58] Galassi M, Davies J, Theiler J, Gough B, Jungman G, Alken P, et al. GNU Scientific Library reference manual. 3rd ed. Network Theory Ltd.; 2009.

[59] Graur D. Molecular and genome evolution. Sunderland, MA: Sinauer; 2016.

[60] Hartl DL. Primer of population genetics and genomics. 4th ed. Oxford University Press; 2020.

[61] Cowperthwaite MC, Meyers LA. How mutational networks shape evolution: Lessons from RNA models. Annu Rev Ecol Evol Syst. 2007;38:203–230.

[62] Tsai C, Kumar S, Ma B, Nussinov R. Folding funnels, binding funnels, and protein function. Protein Sci. 1999;8:1181–1190.

[63] Ma B, Shatsky M, Wolfson HJ, Nussinov R. Multiple diverse ligands binding at a single protein site: A matter of pre-existing populations. Protein Sci. 2002;11:184–197.

[64] Phillips R, Kondev J, Theriot J, Garcia HG. Physical biology of the cell. 2nd ed. New York, NY: Garland Science; 2013.

[65] Monod J, Wyman J, Changeux JP. On the nature of allosteric transitions: A plausible model. J Mol Biol. 1965;12:88–118.

[66] Garcia HG, Kondev J, Orme N, Theriot JA, Phillips R. Thermodynamics of biological processes. In: Johnson ML, Holt JM, Ackers GK, editors. Biothermodynamics, Part D. vol. 492. 1st ed. Academic Press; 2011. p. 27–59.

[67] Changeux JP. Allostery and the Monod-Wyman-Changeux model after 50 years. Annu Rev Biophys. 2012;41:103–133.

[68] Sumedha, Martin OC, Wagner A. New structural variation in evolutionary searches of RNA neutral networks. BioSystems. 2007;90:475–485.

[69] Martin NS, Schaper S, Camargo CQ, Louis AA. Non-poissonian bursts in the arrival of phenotypic variation can strongly affect the dynamics of adaptation. Mol Biol Evol. 2024;41:msae085.

[70] Mäkinen H, Savilammi T, Papakostas S, Leder E, Vøllestad LA, Primmer CR. Modularity facilitates flexible tuning of plastic and evolutionary gene expression responses during early divergence. Genome Biol Evol. 2018;10:77–93.

[71] Espinosa-Soto C, Hernández U, Posadas-García YS. Recombination facilitates genetic assimilation of new traits in gene regulatory networks. Evol Dev. 2021;23:459–473.

[72] Ng ETH, Kinjo AR. Plasticity-led evolution as an intrinsic property of developmental gene regulatory networks. Sci Rep. 2023;13:19380.

[73] Palmer AR. Symmetry breaking and the evolution of development. Science. 2004;306:828–833.

[74] Kulkarni SS, Denver RJ, Gomez-Mestre I, Buchholz DR. Genetic accommodation via modified endocrine signalling explains phenotypic divergence among spadefoot toad species. Nat Commun. 2017;8:993.

[75] Navon D, Male I, Tetrault ER, Aaronson B, Karlstrom RO, Craig Albertson R. Hedgehog signaling is necessary and sufficient to mediate craniofacial plasticity in teleosts. Proc Natl Acad Sci USA. 2020;117:19321–19327.